PERGAMON

Control Engineering Practice 9 (2001) 1095–1106

CONTROL ENGINEERING PRACTICE

www.elsevier.com/locate/conengprac

Integrated design of agile missile guidance and autopilot systems

P.K. Menon[a,*], E.J. Ohlmeyer[b]

[a] *Optimal Synthesis Inc., Research Scientist, 4966 El Camino Real, Suite 108, Los Altos, CA 94022, USA*
[b] *Naval Surface Warfare Center, Code G23, 17320 Dahlgren Road, Dahlgren, VA 22448, USA*

Received 9 April 2001

Abstract

Traditional approach for the design of missile guidance and autopilot systems has been to design these subsystems separately and then to integrate them. Such an approach does not exploit any beneficial relationships between these and other subsystems. A technique for integrated design of missile guidance and autopilot systems using the feedback linearization technique is discussed. Numerical results using a six degree-of-freedom missile simulation are given. Integrated guidance-autopilot systems are expected to result in significant improvements in missile performance, leading to lower weight and enhanced lethality. These design methods have extensive applications in high performance aircraft autopilot and guidance system design.

Keywords: Integrated; Guidance; Autopilot; Feedback linearization

1. Introduction

The evolving nature of the threats to the Naval assets have been discussed in the recent literature (Ohlmeyer, 1996; Bibel, Malyevac, & Ohlmeyer, 1994; Chadwick, 1994; Zarchan, 1995). These research efforts have identified very small miss distance as a major requirement for the next generation missiles used in ship defense against tactical ballistic missiles and sea skimming missiles. Two key technologies that have the potential to help achieve this capability are the development of advanced sensors and methods for achieving tighter integration between the missile guidance, autopilot and fuze-warhead subsystems. This paper presents a preliminary research effort on the integrated design of missile guidance and autopilot system.

Past trend in the missile industry has been to design each subsystem using separate engineering teams and then to integrate them. Modifications are subsequently made to each subsystem in order to achieve the desired weapon system performance. Such an approach can result in excessive design iterations, and may not always exploit synergistic relationships existing between interacting subsystems. This has led to a search for integrated design methods that can help establish design tradeoffs between subsystem specifications early-on in the design iterations. Recent research (Ohlmeyer, 1996) on quantifying the impact of each missile subsystem parameters on the miss distance can serve as the first step towards integrated design of missile guidance and autopilot systems.

Integrated design of the flight vehicle systems is an emerging trend within the aerospace industry. Currently, there are major research initiatives within the aerospace industry, DoD and NASA to attempt interdisciplinary optimization of the whole vehicle design, while preserving the innovative freedom of individual subsystem designers. Integrated design of guidance, autopilot, and fuze-warhead systems represents a parallel trend in the missile technology.

The block diagram of a typical missile guidance and autopilot loop is given in Fig. 1. The target states relative to the missile estimated by the seeker and a state estimator form the inputs to the guidance system. Typical inputs include target position and velocity vectors relative to the missile.

In response to these inputs, and those obtained from the onboard sensors, the guidance system generates acceleration commands for the autopilot. The autopilot uses the guidance commands and sensor outputs to

*Corresponding author. Tel.: +1-650-210-8282; fax: +1-650-210-8289.

E-mail address: menon@optisyn.com (P.K. Menon).

0967-0661/01/$ - see front matter
PII: S0967-0661(01)00082-X

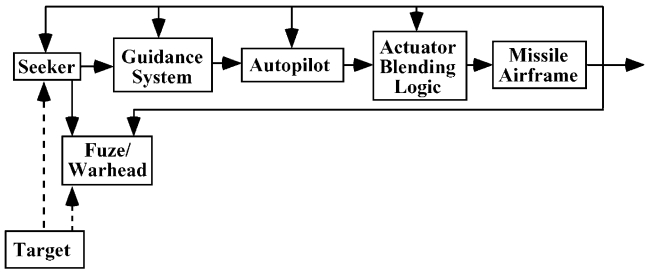

Fig. 1. Block diagram of an advanced missile guidance, autopilot, and fuze/warhead systems.

generate commands for the actuator blending logic, which optimally selects a mix of actuators to be used at the given flight conditions. The fuse-warhead subsystem uses the relative location of the target with respect to the missile as the input and responds in such a way as to maximize the warhead effectiveness.

Each of these subsystems has interactions that can be exploited to optimize the performance of the missile system. For instance, missiles with higher accuracy guidance and autopilot systems can employ smaller warheads. Guidance laws that have anticipatory capabilities can reduce the autopilot time response requirements. High bandwidth autopilot can make the guidance system more effective. High quality actuator blending logic can similarly lead to more accurate fuel conservative maneuvers that can enhance the autopilot performance. Similarly, the seeker field of view and speed of response depend on the target agility, and the response of missile guidance and autopilot system.

Traditional approach for designing the missile autopilot and guidance systems has been to neglect these interactions and to treat individual missile subsystems separately. Designs are generated for each subsystem and these subsystems are then assembled together. If the overall system performance is unsatisfactory, individual subsystems are re-designed to improve the system performance. While this design approach has worked well in the past, it often leads to the conservative design of the on-board systems, leading to a heavier, more expensive weapon system.

"Hit-to-kill" capabilities required in the next generation missile system will require a more quantitative design approach in order to exploit synergism between various missile subsystems, and thereby guaranteeing the weapon system performance. Integrated system design methods available in the literature (Garg, 1993; Menon & Iragavarapu, 1995) can be tailored for designing the missile subsystems.

This paper presents the application of the feedback linearization method for the integrated design of missile guidance and autopilot systems. Integration of actuator blending logic (Menon & Iragavarapu, 1998) and other subsystems will be considered during future research efforts. The present research employs a six degree-of-freedom nonlinear missile model, and a maneuvering point-mass target model. These models are discussed in Section 2. Section 2 also lists the general performance requirements of the integrated guidance-autopilot system design.

Section 3 presents the details of the integrated guidance-autopilot system design and performance evaluation. Conclusions from the present research are given in Section 4.

2. Missile model

A nonlinear six degrees-of-freedom missile model is used for the present research. This model is derived from a high fidelity simulation developed under a previous research effort (Menon & Iragavarapu, 1996), and will be further discussed in Section 2.1. The guidance-autopilot system development will include a point-mass target model performing weaving maneuvers. The equations of motion for the target will be given in Section 2.2. Section 2.3 will discuss the performance requirements of the integrated guidance-autopilot system.

2.1. Six degrees of freedom missile model

A body coordinate system and an inertial coordinate system are used to derive the equations of motion. These coordinate systems are illustrated in Fig. 2. The origin of the body axis system is assumed to be at the missile center of gravity. The X_B-axis of the body axis system points in the direction of the missile nose, the Y_B-axis points in the starboard direction, and the Z_B-axis completes the right-handed triad. The missile position and attitude are defined with respect to an earth-fixed inertial frame. The origin of the earth-fixed coordinate system is located at the missile launch point, with the X-axis pointing towards the initial location of the target, and the Z-axis pointing along the local gravity vector.

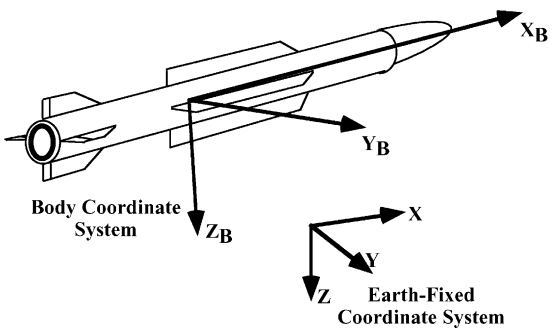

Fig. 2. Missile coordinate systems.

The Y-axis direction completes the right-handed coordinate system.

The translational and rotational dynamics of the missile are described by the following six nonlinear differential equations:

$$\dot{U} = -\frac{\bar{q}s}{m} C_x - WQ + VR + \frac{F_{xg}}{m},$$

$$\dot{V} = -\frac{\bar{q}s}{m} C_y - UR + WP + \frac{F_{yg}}{m},$$

$$\dot{W} = -\frac{\bar{q}s}{m} C_z - VP + UQ + \frac{F_{zg}}{m},$$

$$\dot{P} = \frac{1}{I_x} C_l \bar{q} s l, \quad \dot{Q} = C_m \bar{q} s l - \frac{(I_x - I_z)}{I_y} PR,$$

$$\dot{R} = C_n \bar{q} s l - \frac{(I_y - I_x)}{I_y} PQ.$$

In these equations, U, V, W are the velocity components measured in the missile body axis system; P, Q, R are the components of the body rotational rate; F_{xg}, F_{yg}, F_{zg} are the gravitational forces acting along the body axes; and I_x, I_y, I_z are the vehicle moments of inertia. The variable s is the reference area and l the reference length.

For the present research, it is assumed that the missile body axes coincide with its principal axes. The aerodynamic force and moment coefficients C_x, C_y, C_z, C_l, C_m, C_n are given as table lookup functions with respect to Mach number M, angle of attack α, angle of sideslip β, pitch fin deflection δ_Q, yaw fin deflection δ_R, and the roll fin deflection δ_P. These coefficients have the functional form:

$$\begin{aligned} C_x &= C_{x0}(M) + C_{x\alpha\beta}(M,\alpha,\beta) + C_{xh}(M,h) \\ &\quad + C_{x\delta_T}(M,\alpha,\beta), \\ C_y &= C_{y0}(M,\alpha,\beta) + C_{y\delta_P}(M,\alpha,\beta)\delta_P + C_{y\delta_Q}(M,\alpha,\beta)\delta_Q \\ &\quad + C_{y\delta_R}(M,\alpha,\beta)\delta_R, \\ C_z &= C_{z0}(M,\alpha,\beta) + C_{z\delta_P}(M,\alpha,\beta)\delta_P + C_{z\delta_Q}(M,\alpha,\beta)\delta_Q \\ &\quad + C_{z\delta_R}(M,\alpha,\beta)\delta_R, \end{aligned}$$

$$\begin{aligned} C_l &= C_{l0}(M,\alpha,\beta) + C_{lP}(M)\frac{PD_r}{2v} + C_{l\delta_P}(M,\alpha,\beta)\delta_P \\ &\quad + C_{l\delta_Q}(M,\alpha,\beta)\delta_Q + C_{l\delta_R}(M,\alpha,\beta)\delta_R, \\ C_m &= C_{m0}(M,\alpha,\beta) + C_{mP}(M)\frac{PD_r}{2v} + C_{m\delta_P}(M,\alpha,\beta)\delta_P \\ &\quad + C_{m\delta_Q}(M,\alpha,\beta)\delta_Q + C_{m\delta_R}(M,\alpha,\beta)\delta_R, \\ C_n &= C_{n0}(M,\alpha,\beta) + C_{nP}(M)\frac{PD_r}{2v} + C_{n\delta_P}(M,\alpha,\beta)\delta_P \\ &\quad + C_{n\delta_q}(M,\alpha,\beta)\delta_Q + C_{n\delta_R}(M,\alpha,\beta)\delta_R. \end{aligned}$$

The missile speed V_T, Mach number M, dynamic pressure $\bar{q}$, angle of attack α, and the angle of sideslip β are defined as

$$V_T = \sqrt{U^2 + V^2 + W^2}, \quad M = V_T/a, \quad \bar{q} = \frac{1}{2}\rho V_T^2,$$

$$\alpha = \tan^{-1}\left(\frac{W}{U}\right), \quad \beta = \tan^{-1}\left(\frac{V}{U}\right).$$

A cruciform missile is considered in the present study. The control moments in pitch and yaw axes are produced by deflecting the corresponding fin deflections, while the roll control is achieved by differential deflection of the pitch/yaw fins. A fin interconnect logic is used to obtain the desired roll fin deflection from the pitch/yaw fins.

The missile position with respect to the earth-fixed inertial coordinate system can be described by using a coordinate transformation matrix T_{IB} between the body frame and the inertial frame as

$$\begin{bmatrix} \dot{X}_M^I \\ \dot{Y}_M^I \\ \dot{Z}_M^I \end{bmatrix} = T_{IB} \begin{bmatrix} U \\ V \\ W \end{bmatrix}.$$

The superscript I denotes quantities in the inertial frame, and the subscript M denotes the missile position/velocity components. The coordinate transformation matrix with respect to the Euler angles ψ, θ, ϕ is

$$T_{IB} = \begin{bmatrix} \cos\theta\cos\psi & \sin\phi\sin\theta\cos\psi - \cos\phi\sin\psi & \cos\phi\sin\theta\cos\psi + \sin\phi\sin\psi \\ \cos\theta\sin\psi & \sin\phi\sin\theta\sin\psi + \cos\phi\cos\psi & \cos\phi\sin\theta\sin\psi - \sin\phi\cos\psi \\ -\sin\theta & \sin\phi\cos\theta & \cos\phi\cos\theta \end{bmatrix}.$$

Yaw (ψ), pitch (θ), roll (ϕ) Euler angle sequence is used to derive this transformation matrix. The Euler angle rates with respect to the body rotational rates are given by the expressions:

$$\dot{\theta} = Q\cos\phi - R\sin\phi,$$

$$\dot{\phi} = P + Q\sin\phi\tan\theta + R\cos\phi\tan\theta,$$

$$\dot{\psi} = (Q\sin\phi + R\cos\phi)\sec\theta.$$

Since the missile seeker defines the target position relative to the missile body coordinate system, it is desirable to describe the relative position and velocity of the target with respect to the instantaneous missile body axis system. The position of the target with respect to the missile in the missile body frame is given by

$$\begin{bmatrix} x_r^M \\ y_r^M \\ z_r^M \end{bmatrix} = T_{IB}^{\mathrm{T}} \begin{bmatrix} x_T^I - x_M^I \\ y_T^I - y_M^I \\ z_T^I - z_M^I \end{bmatrix}.$$

The subscript r denotes relative quantities. $\begin{bmatrix} x_T^I & y_T^I & z_T^I \end{bmatrix}^{\mathrm{T}}$ is the target position vector in the

inertial frame. The target velocity vector relative to the missile body frame is given by

$$\begin{bmatrix} U_r^M \\ V_r^M \\ W_r^M \end{bmatrix} = T_{IB}^{\mathrm{T}} \begin{bmatrix} \dot{x}_T^I \\ \dot{y}_T^I \\ \dot{z}_T^I \end{bmatrix} - \begin{bmatrix} U \\ V \\ W \end{bmatrix} - \begin{bmatrix} Qz_r^M - Ry_r^M \\ Rx_r^M - Pz_r^M \\ Py_r^M - Qx_r^M \end{bmatrix}.$$

The main advantage of describing the target position relative to the missile in the rotating coordinate system is that it circumvents the need for computing the Euler angles required in the transformation matrix during guidance-autopilot computations.

Second-order fin actuator dynamics from Menon and Iragavarapu (1996) is incorporated in the missile model. However, due to their fast speed of response, these models are not used for integrated guidance-autopilot logic development. During future work, the actuator blending logic developed in a previous research study (Menon & Iragavarapu, 1998) will be used to integrate the reaction jet actuators in the integrated guidance-autopilot loop.

Although the measurements available onboard the missile are limited, the present research will assume that all the measurements required for the implementation of the integrated guidance-autopilot are available.

2.2. Target model

Two different target models are considered in the present research. The first is a maneuvering target that executes sinusoidal weaving trajectories, with 0.5 Hz frequency with a 5 g amplitude. Thus, the maneuvering target model has the form

$$\dot{U}_T = 0, \quad \dot{V}_T = A\sin(\omega t), \quad \dot{W}_T = 0.$$

The second is a non-maneuvering target with a model

$$\dot{U}_T = \dot{V}_T = \dot{W}_T = 0.$$

The target trajectory is obtained by integrating the following equations:

$$\begin{bmatrix} \ddot{x}_T^I \\ \ddot{y}_T^I \\ \ddot{z}_T^I \end{bmatrix} = T_{IB} \begin{bmatrix} \dot{U}_T \\ \dot{V}_T \\ \dot{W}_T \end{bmatrix}.$$

2.3. Integrated guidance-autopilot performance requirements

In traditional flight control systems, the guidance law uses the relative missile/target states to generate acceleration commands. The acceleration commands are generated with the assumption that the missile rotational dynamics is fast enough to be considered negligible. If perfectly followed, these acceleration commands will result in target interception. The autopilot tracks the acceleration commands by changing the missile attitude to generate angle of attack and angle of sideslip using fin deflections and/or moments generated using the reaction jet thrust.

These two functions are combined in integrated guidance-autopilot. Integrated guidance-autopilot uses the target states relative to the missile to directly generate fin deflections that will result in target interception. In addition to achieving target interception, the integrated guidance-autopilot has the responsibility for ensuring the internal stability of the missile dynamics. Some of the general performance guidelines used during the present research for integrated guidance-autopilot system design are that:

1. It must intercept maneuvering targets with very small miss distances.
2. It must maintain the roll rate near zero throughout the engagement.
3. It must be capable of intercepting the target with a desired terminal aspect angle. The aspect angle may be defined in various ways. For purposes of this research, it is defined as the angle between the missile velocity vector and the target velocity vector at intercept. It is obvious that a good estimate of the target velocity vector with respect to the missile is essential for reliably implementing the terminal aspect angle constraint.
4. It must stabilize all the states of the missile.
5. It must achieve its objectives while satisfying the position and rate limits on the fin/reaction jet actuators.

Performance requirements other than the terminal aspect angle constraint are standard in every missile design problem. The terminal aspect angle constraint can be satisfied in several different ways. Firstly, the guidance-autopilot logic can be explicitly formulated to meet the terminal aspect angle constraint. While this is the most direct approach, the resulting formulation may be analytically intractable. The approach followed in the present research is based on ensuring that the relative missile-target lateral velocity component at interception will be a fixed fraction of the relative missile-target longitudinal velocity component. This way, the terminal aspect angle constraint is converted into a constraint on the relative missile/target lateral velocity component at the final time. For the present study, the terminal aspect angle constraint requires the integrated guidance-autopilot system to orient the missile velocity vector as closely parallel as possible to the target velocity vector at interception.

Missile/target models discussed in this section form the basis for the development of integrated guidance-autopilot logic in the following section.

3. Integrated design using the feedback linearization technique

The feedback linearization technique (Brockett 1976; Isidori 1989; Marino & Tomei, 1995) has evolved over the past two decades as a powerful methodology for the design of nonlinear control systems. Several papers describing the application of this technique to flight vehicles have been reported (Menon, Badgett, Walker, & Duke, 1987; Menon, Iragavarapu, & Ohlmeyer, 1999). The key idea in this technique is the transformation of the system dynamics into the Brunovsky canonical form (Kailath, 1980). In this form, all the system nonlinearities are "pushed" to the input, and the system dynamics appears effectively as chains of integrators.

In order to motivate subsequent discussions, the feedback linearization process will be outlined for a single-input, multi-state system in the following. If the nonlinear system dynamics is given the form

$$\dot{x} = f(x) + g(x)u,$$

then, the transformed model in Brunovsky's canonical form is: $\dot{z} = Az + Bv$, with

$$A = \begin{bmatrix} 0 & 1 & 0 & \cdots & 0 \\ 0 & 0 & 1 & \cdots & 0 \\ \vdots & \vdots & \vdots & \ddots & \vdots \\ 0 & 0 & 0 & \cdots & 1 \\ 0 & 0 & 0 & \cdots & 0 \end{bmatrix}, \quad B = \begin{bmatrix} 0 \\ 0 \\ \vdots \\ 0 \\ 1 \end{bmatrix},$$

z is the transformed state. The variable $v = F(x) + G(x)u$ is often termed as the pseudo control variable, with $F(x)$ and $G(x)$ being nonlinear functions of the state variables. The transformed system is in linear, time-invariant form with respect to the pseudo control variable. This procedure can be extended to multi-input nonlinear dynamic systems.

The transformation of a nonlinear dynamic system into Brunovsky's canonical form is achieved through repeated differentiation of the system state equations. While symbolic manipulations are feasible in simple problems, this process can be difficult and error prone in more complex practical problems. Moreover, since a large portion of the missile model is in the form of table lookups, the transformation methodology based on symbolic manipulations is impractical. A general-purpose nonlinear toolbox is commercially available to carry out the feedback linearization process in applications where the system dynamic model is specified in the form of a simulation (Menon et al., 2000a). This software tool will be used in the present research.

After the system is transformed into the Brunovsky canonical form, any linear control design method can be applied to derive the pseudo control variable v. The Linear Quadratic design technique (Bryson & Ho, 1975) will be employed for the design of the pseudo control loop in the present research. Actual control, u can then be recovered from the pseudo control variables using the inverse transformation

$$u = G^{-1}(x)\{v - F(x)\}.$$

Note that the closed loop properties of the resulting nonlinear controller will be identical to the pseudo control system if the nonlinearities are exactly known. However, as a practical matter, uncertainties will exist in the computation of the system nonlinearities $F(x)$ and $G(x)$. Consequently, the actual system performance will be different from that of the pseudo control loop. The closed-loop nature of the controller will tend to ameliorate the sensitivity of the dynamic system response to these perturbations.

In systems where the control variables do not appear linearly in the system dynamics, additional steps may be required to transform the system into the desired form. For instance, if the system is specified in the form

$$\dot{x} = h(x, u),$$

it can be augmented with integrators at the input to convert it into the standard form. Thus, the augmented model

$$\dot{x} = h(x, u), \quad \dot{u} = u_c,$$

is in the standard form with u_c being the new control vector. The feedback linearization methodology can then be carried out as indicated at the beginning of this section.

3.1. Missile model in feedback linearized form

In order to apply the feedback linearization technique for integrated guidance-autopilot system, the missile equations of motion presented in Section 2 have to be transformed into the Brunovsky canonical form. The first step in this transformation is the identification of the dominant relationships in the system dynamics.

These relationships describe the main cause-effect relationships in the system dynamics, and can also be described using the system *Digraph* (Siljak, 1991). For instance, in the roll channel, the dominant relationships are: the roll fin deflection primarily influences the roll rate, which in turn affects the roll attitude. Similarly, in the pitch axis, the pitch fin deflection causes a pitch rate, which generates the normal acceleration. The normal acceleration in turn leads to a reduction of the separation between the missile and the target. The cause-effect relationship in the yaw channel is identical to the pitch channel. These dominant relationships can

be summarized as

$$\delta_P \to P \to \phi,$$
$$\delta_Q \to Q \to W_r^M \to z_r^M,$$
$$\delta_R \to R \to V_r^M \to y_r^M.$$

Note that in addition to these dominant effects, the missile dynamics includes significant coupling between the pitch, yaw and roll axes.

Using these relationships, together with permissible perturbations in the system states, the nonlinear synthesis software (Menon et al., 2000a) can automatically construct a feedback linearized dynamic system from a simulation model of the missile at every value of the state. This process is achieved by numerically differentiating the system simulation model, and using numerical linear algebra functions (Anderson et al., 1999). The transformed system can then be used to design the integrated guidance-autopilot system.

3.2. LQR—feedback linearization design of integrated guidance-autopilot system

As stated at the beginning of Subsection 3.1, once the system dynamics is transformed into the feedback linearized form, any linear system design technique can be used to design the integrated guidance-autopilot logic. The infinite-time horizon LQR technique (Bryson & Ho, 1975) is employed in the present research. In this technique, the designer has the responsibility for selecting a positive semi-definite state weighting matrix, and a positive definite control weighting matrix. The state and control weighting matrices can be chosen based on the maximum permissible values (Bryson & Ho, 1975) of the fin deflections and the missile state variables.

Since the feedback linearized system dynamics is linear and time invariant, one control law design is adequate to guarantee closed-loop system stability. However, in order to minimize the miss distance, it is desirable that the missile response becomes more agile as it gets closer to the target. This can be achieved by using lower state weights when the missile is far away from the target, and as the missile approaches the target, the state weights can be tightened. A reverse strategy can be used for the control weighting matrix: higher magnitudes when the missile is far from the target, and smaller magnitudes as the missile approaches the target. In this way, the closed-loop system response can be tailored to approximate the behavior of a finite time-horizon integrated guidance-autopilot law. Note that such range or time-to-go based scheduling strategy is automatically built into more traditional guidance laws like the proportional navigation and augmented proportional navigation guidance laws (Bryson & Ho, 1975). In the present research, the state weighting matrix is defined as an inverse function of the range-to-go. The constant of proportionality is chosen based on the permissible initial transient of the missile.

Note that this approach will require the online solution of an algebraic Riccati equation. Recent research has established (Menon, Lam, Crawford, & Cheng, 2000b) that for problems of the size encountered in the missile guidance-autopilot problems, the corresponding algebraic Riccati equation can be solved at sample rates in excess of 1 kHz on commercial off-the-shelf processors.

3.3. Command generation

Since the guidance-autopilot logic is an infinite time formulation, when faced with an error, it will immediately respond to correct all the error. This can lead to actuator saturation followed by large transients in the state variables, with the potential for the closed-loop system to go unstable. On the other hand, slowing the system down to prevent actuator saturation can lead to sluggish response, with the possibility for large miss distances. The use of a command generator can alleviate these difficulties. The command generator will allow a control system to use high loop gains while providing a saturation-free closed-loop system response. Additionally, the command generator will enable the guidance-autopilot system to meet the terminal aspect angle requirements. This section will outline a command generator used in the present research.

The design flexibility available with the use of a command shaping network at the input has been amply demonstrated in linear system design literature (Wolovich, 1994). This two degree-of-freedom design philosophy employs a command shaping network to obtain the desired tracking characteristics, and a feedback compensator is used to achieve the desired closed-loop system stability and robustness characteristics. These two subsystems can be used to achieve overall design objectives without sacrificing stability, robustness or the tracking response of the closed-loop system. From an implementation point of view, the two degree-of-freedom design process allows high gain control laws that will not saturate the actuators in the presence of large input commands.

In the integrated guidance-autopilot problem, the command generator uses the current target position and velocity components with respect to the missile body frame, desired boundary conditions and expected point of interception to synthesize a geometric command profile. The command profile is re-computed at each time instant, allowing for the correction of intercept point prediction errors made during the previous step. Such an approach will distribute the control power requirements over the interception time, thereby

providing a fast responding closed-loop system that does not produce unnecessary actuator saturation.

The command profile can be computed from the initial conditions and the interception requirements. The initial conditions on the missile position and velocity are specified, and the terminal position of the missile must coincide with the target. In the case of a terminal aspect angle requirement, the terminal velocity components may also be specified. Since there are four conditions to be satisfied, a cubic polynomial is necessary to represent the command profile. Note that if the terminal aspect angle requirement is absent, a quadratic polynomial is sufficient for generating commands. The independent variable of the cubic polynomial can be chosen as the state variable not being controlled, namely, the position difference between the missile and the target along the X-body axis of the missile. Additionally, since the desired final miss distance is zero, the leading term in the cubic polynomial can be dropped. With this, the commanded trajectory profiles will be of the form:

$$y_{rc}^M = a_1 x_r^M + a_2[x_r^M]^2 + a_3[x_r^M]^3,$$
$$z_{rc}^M = b_1 x_r^M + b_2[x_r^M]^2 + b_3[x_r^M]^3.$$

Fig. 3 illustrates a typical commanded trajectory profile. The coefficients a_1, a_2, a_3, b_1, b_2, b_3 can be computed using the remaining boundary conditions.

Note that the command profiles will not require the specification of time-to-go, but will require the specification of the closing rate along the X-body axis. Target interception will be achieved if the integrated guidance-autopilot logic closely tracks the commands. In case of agile targets, it may be useful to include a certain amount of anticipatory characteristics in the command generator. This will effectively introduce additional "phase lead" in the integrated guidance-autopilot loop, potentially resulting in decreased miss distances. These and other advanced command generation concepts will be investigated during future research.

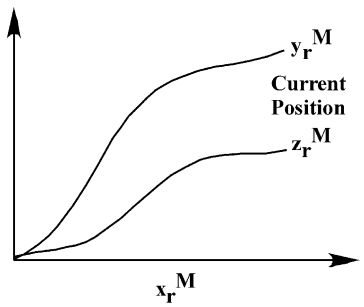

Fig. 3. Commanded trajectory profile in the missile Y-axis.

3.4. Integrated guidance-autopilot system performance evaluation

As discussed in the previous sections, the integrated guidance-autopilot system consists of a command generator, and feedback linearized guidance-autopilot logic. A schematic block diagram of the integrated guidance-autopilot system is given in Fig. 4.

A six degree-of-freedom missile simulation set up during an earlier research (Menon & Iragavarapu, 1996) is used to evaluate the performance of the integrated guidance-autopilot system. This simulation incorporates a generic nonlinear missile model, together with sensor/actuator dynamics. A point-mass target model is included in all the simulation runs. Euler integration method with a step size of 1 ms is used in all the simulation.

The engagement scenarios illustrated here assume that the missile is flying at an altitude of 10,000 ft, and at a Mach number of 4.5. The target is flying at Mach 1. The results for two engagement scenarios will be given in the following. In each case, the guidance-autopilot objective is to intercept the target while making the missile velocity vector parallel to the target velocity vector at interception.

4. Non-maneuvering target

The first scenario chosen to illustrate the performance of the integrated guidance-autopilot system is that of intercepting a target flying at 11,000 ft altitude, 14,000 ft down range, and 20,000 ft cross range. The missile/target trajectories in the vertical and horizontal plane are given in Fig. 5. The unusual nature of the

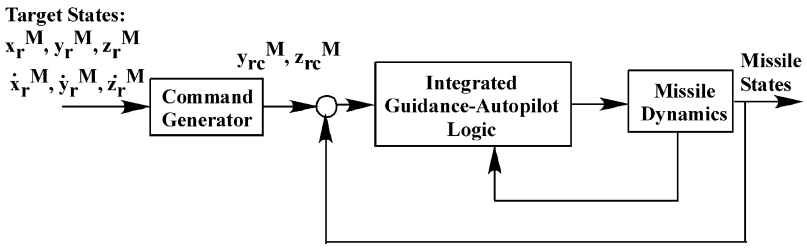

Fig. 4. Integrated guidance-autopilot system.

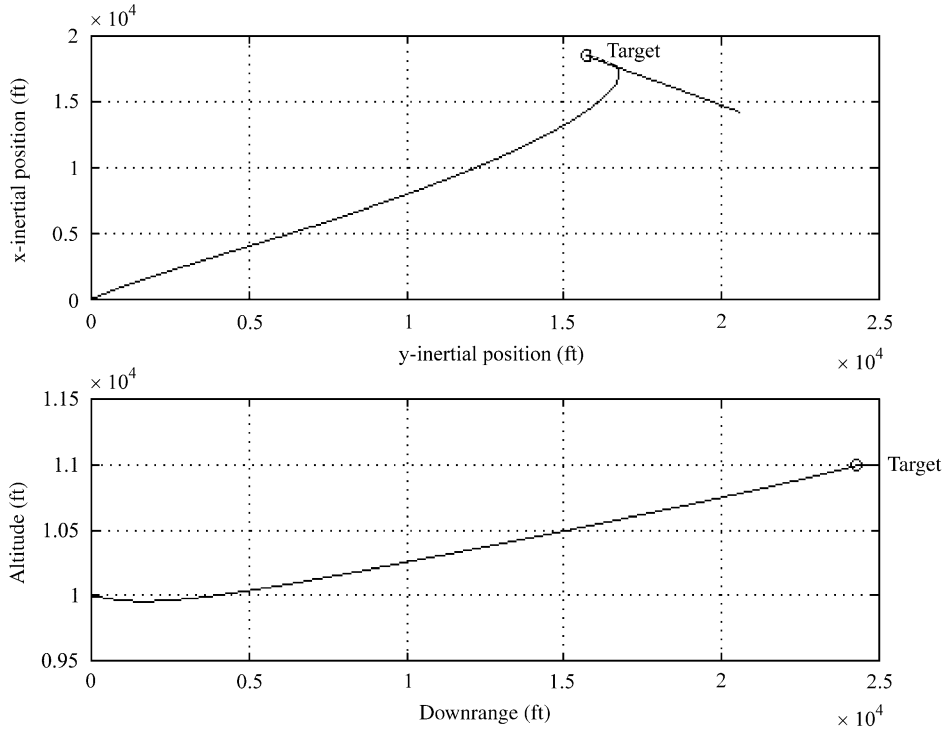

Fig. 5. Interception of a non-maneuvering target.

horizontal-plane trajectory arises from the terminal aspect angle constraint.

The interception occurred at about 7 s, with a miss distance of about 20 ft. It can be observed from the trajectories that the terminal aspect angle constraint has been satisfied. Analysis has shown that the observed miss distance arises primarily due to the terminal aspect angle requirements, and not because of any inherent limitations of the guidance-autopilot formulation. Thus, in order to meet the terminal aspect angle constraint, the integrated control system drove the Y_b error to zero a few milliseconds before driving the Z_b error to zero. Note that this miss distance can be reduced through the use of an improved command generator, perhaps including a certain amount of "lead". Additional refinements include the use of integral feedback on the two position components. These improvements will be pursued during future research.

The missile angle of attack and angle of sideslip corresponding to this intercept scenario are given in Fig. 6. The missile roll, pitch, yaw rate histories during the first second of the engagement are presented in Fig. 7. After the initial transient, the body rates remain zero until target intercept. The missile aerodynamic model used in the present research contains strong coupling effects between the pitch/yaw axes and the roll axis in the presence of angle of attack and angle of sideslip. The effect of this coupling can be observed in the roll rate history. During the last second, the pitch and yaw rates increase to significantly higher values to provide the acceleration components required to achieve target interception. Fin deflections corresponding to Fig. 7 are given in Fig. 8.

5. Weaving target

A weaving target model discussed in Section 2 is used to evaluate the response of the integrated guidance-autopilot system. The missile initial conditions were identical to the previous case. The target is assumed to be located at 16,000 ft in down range, 5000 ft in cross range, and 10,000 ft altitude. A weaving amplitude of 5g's, with a frequency of 0.5 Hz is introduced in the horizontal plane.

The missile-target trajectories in the horizontal and the vertical planes are presented in Fig. 9. The interception required about 5.5 s, and the terminal miss distance was about 25 ft. The near parallel orientation of the missile and target velocity vectors at the intercept point can be observed in this figure.

As in the previous case, the miss distance could be largely attributed to the differences in performance between the vertical and horizontal channels. Numerical experiments have shown that improved state-control weight selection will produce significant improvements in the miss distance. A command generator including some lead can also contribute towards reducing the miss distance.

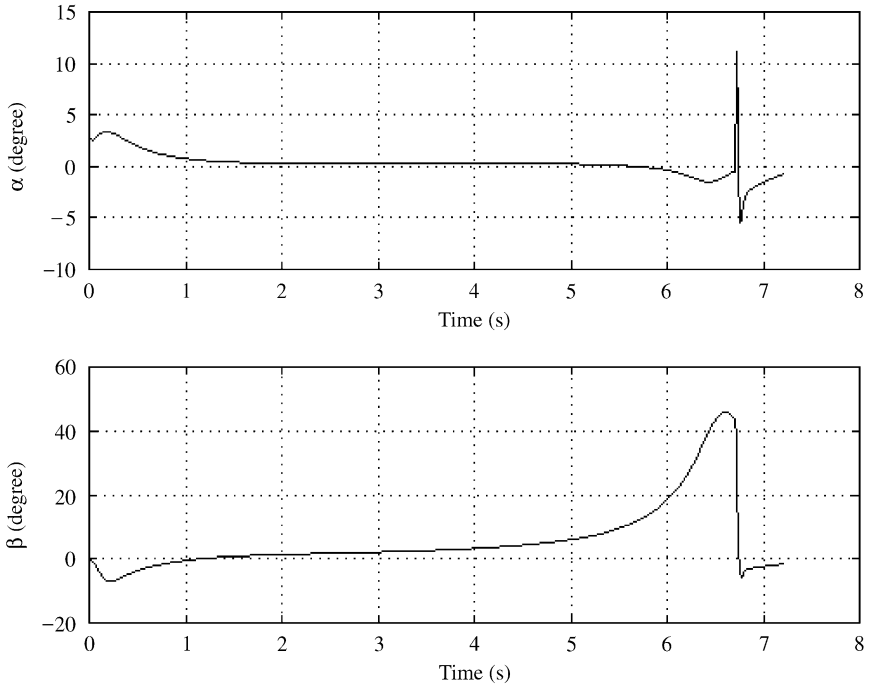

Fig. 6. Temporal evolution of missile angle of attack and angle of sideslip.

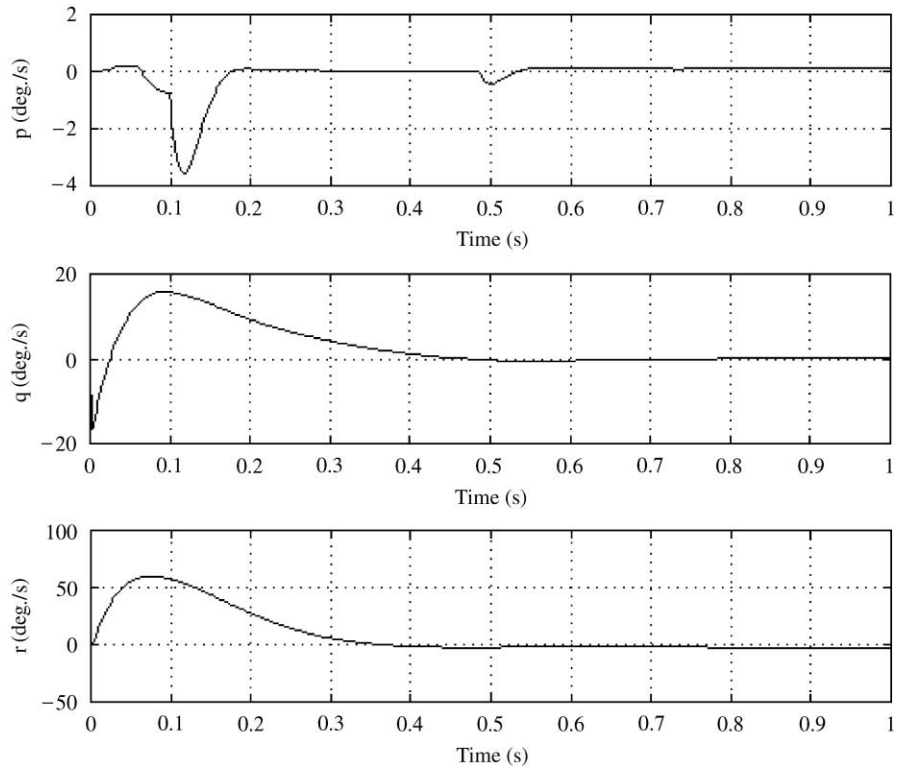

Fig. 7. Roll, pitch, yaw rate histories.

The angle of attack and angle of sideslip histories corresponding to this engagement are illustrated in Fig. 10. Roll, pitch, yaw body rates during the first second of the engagement are illustrated in Fig. 11. Corresponding fin deflections are given in Fig. 12.

As in the previous engagement scenario, due to the reactive nature of the guidance-autopilot logic, most of

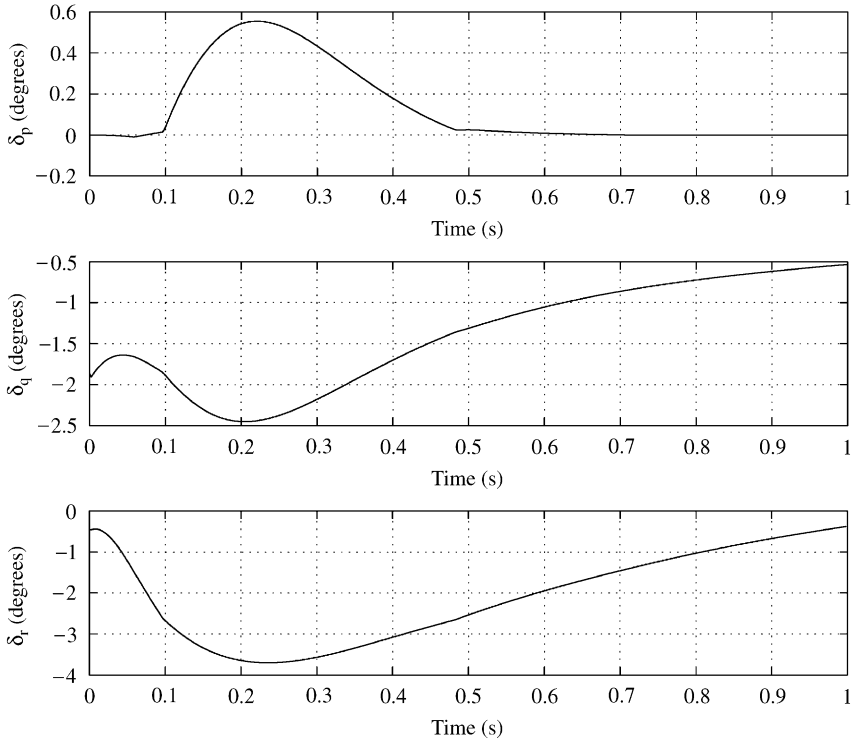

Fig. 8. Fin deflection histories.

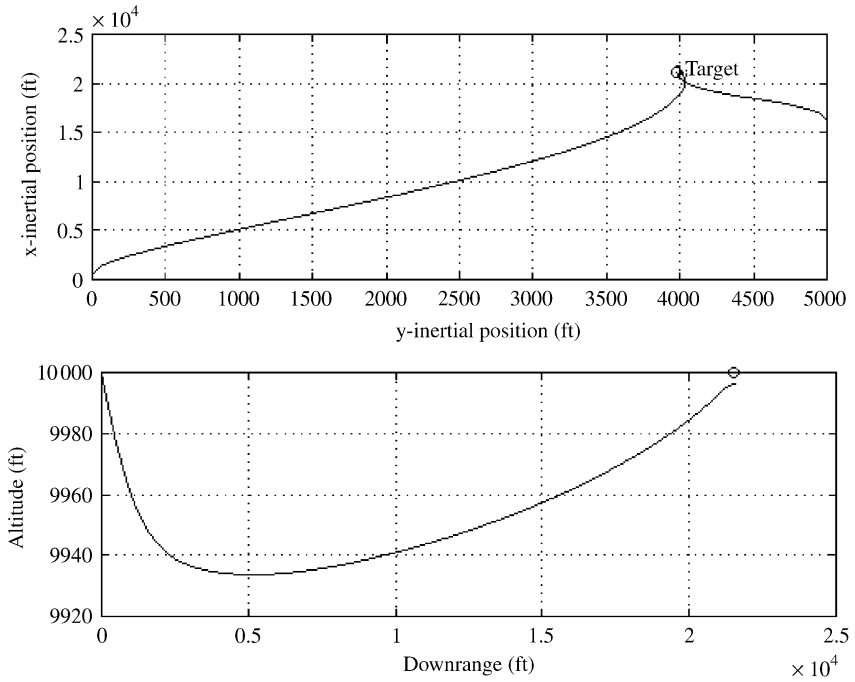

Fig. 9. Interception of a weaving target.

the control activity is at the beginning of the engagement. This indicates that additional improvements may be required in scheduling the state-control weighting matrices with respect to time-to-go or range-to-go to make the guidance-autopilot system respond more uniformly throughout the engagement.

6. Conclusions

Feedback linearization method for designing integrated guidance-autopilot systems for ship defense missiles was discussed this paper. The integrated missile guidance-autopilot system design was formulated as an

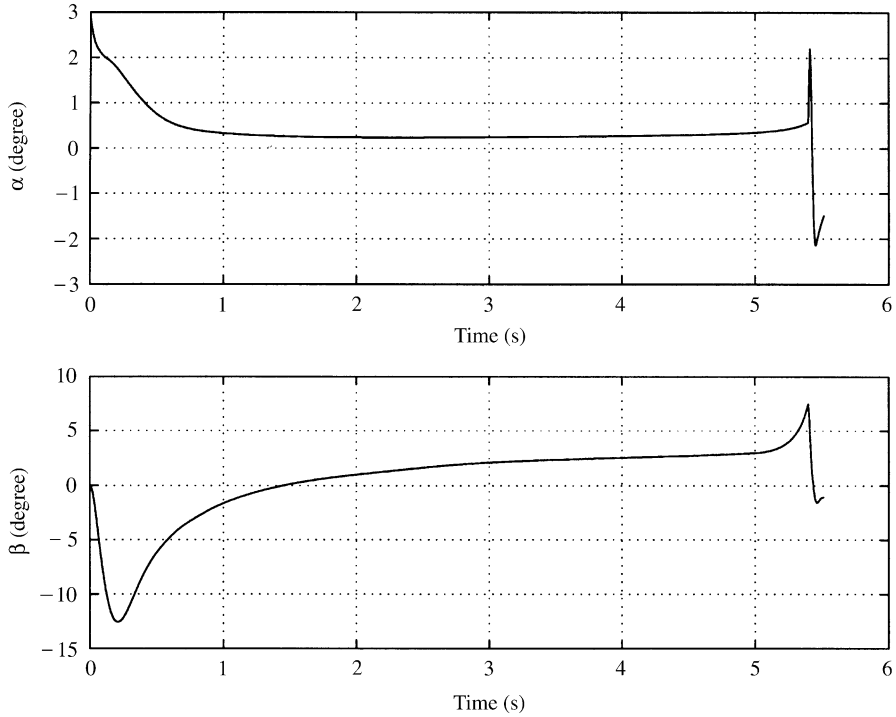

Fig. 10. Angle of attack and angle of sideslip histories.

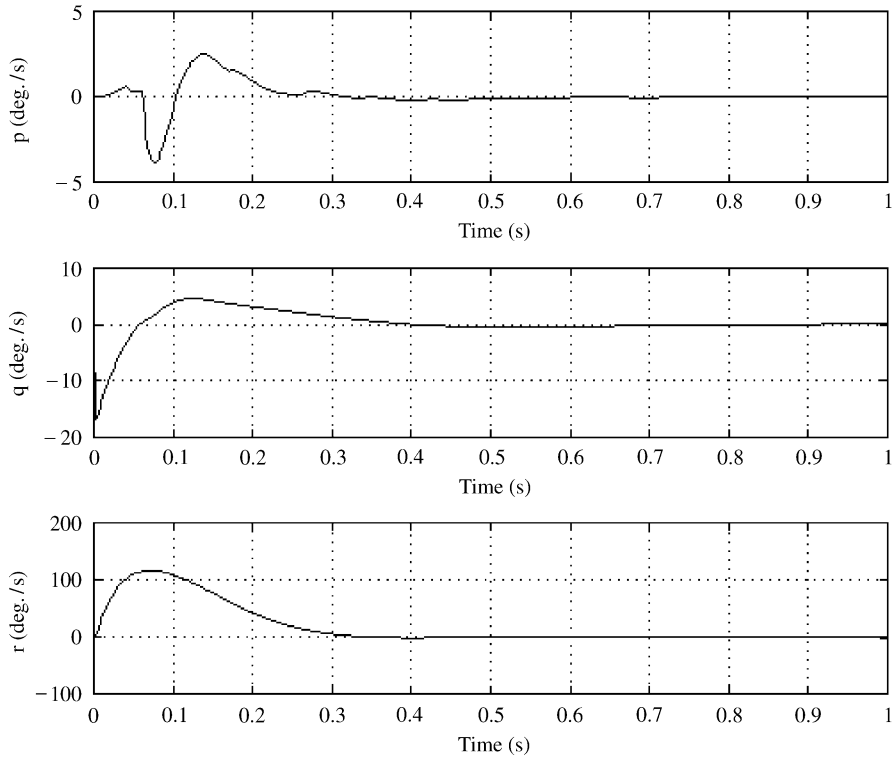

Fig. 11. Roll, pitch, yaw rate histories.

infinite time-horizon optimal control problem. The need for a command generator was motivated, and a cubic command generator development was presented. Introduction of the command generator allowed the control loop to use high gain without resulting in actuator saturation. The command generator was also shown to be useful for meeting terminal aspect angle constraints. The integrated guidance-autopilot logic performance was demonstrated in a nonlinear six degree-of-freedom missile simulation for a non-maneuvering target and a

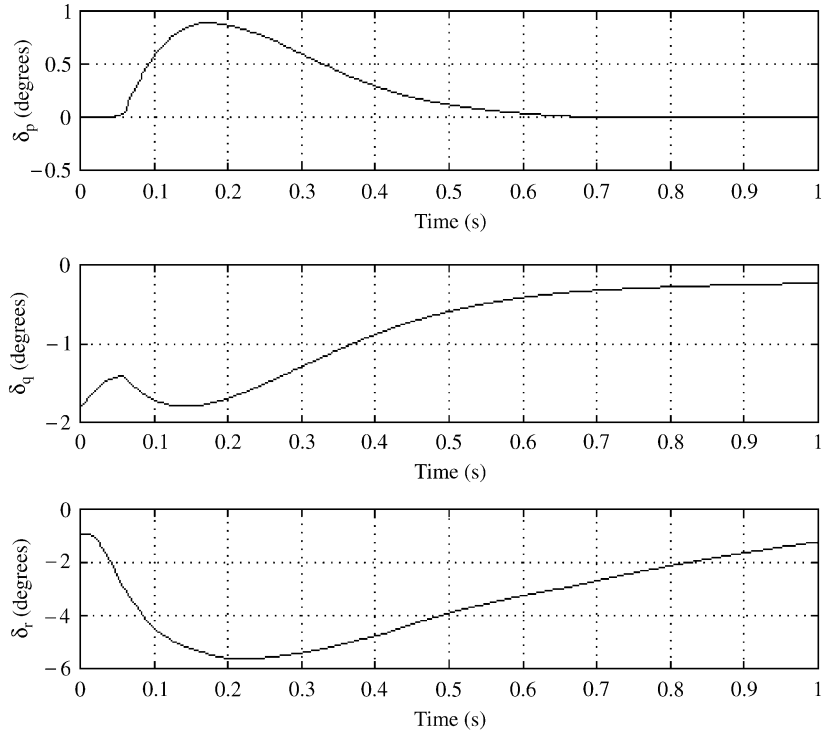

Fig. 12. Fin deflection histories.

weaving target. Methods for further refining the integrated guidance-autopilot logic were discussed.

The analysis and numerical results presented in this paper amply demonstrate the feasibility of designing integrated guidance-autopilot systems for the next generation high-performance missile systems. Integrated design methods have the potential for enhancing missile performance while simplifying the design process. This can result in a lighter, more accurate missile system for effective defense against various threats expected in the future. Future research will examine improvements in the formulation of the integrated guidance-autopilot design problem and the system robustness.

References

Anderson, E., Bai, Z., Bischof, C., Blackford, S., Demmel, J., Dongarra, J., Du Croz, J., Greenbaum, A., Hammarling, S., McKenney, A., & Sorensen, D. (1999). *LAPACK user's guide*. Philadelphia, PA: Society for Industrial and Applied Mathematics (*SIAM*).

Bibel, J. E., Malyevac, D. S., & Ohlmeyer, E. J, (1994). Robust flight control for surface launched tactical missiles. *Naval Surface Warfare Center Dahlgren Division Technical Digest*, September.

Brockett, R. W. (1976). Nonlinear Systems and Differential Geometry. *Proceedings of the IEEE*, *64*(1), 61–72.

Bryson, A. E., & Ho, Y. C. (1975). *Applied optimal control*. New York: Hemisphere.

Chadwick, W. R., (1994). Reentry flight dynamics of a non-separating tactical ballistic missile. *Proceedings of the AIAA/BMDO Interceptor Technology Conference*. San Diego, CA.

Garg, S. (1993). Robust integrated flight/propulsion control design for a STOVL aircraft using H-infinity control design techniques. *Automatica*, *29*(1), 129–145.

Isidori, A. (1989). *Nonlinear control systems*. Berlin: Springer.

Kailath, T. (1980). *Linear systems*. Englewood Cliffs, NJ: Prentice-Hall.

Menon, P. K., Badgett, R., Walker, R. A., & Duke, E. L. (1987). Nonlinear flight test trajectory controllers for aircraft. *Journal of Guidance, Control and Dynamics*, *10*(1), 67–72.

Menon, P. K., & Iragavarapu, V. R. (1995). Computer-Aided Design Tools for Integrated Flight/Propulsion Control System Synthesis. Final Report Prepared under NASA Lewis Research Center Contract No. NAS3-27578.

Menon, P. K., & Iragavarapu, V. R. (1996). Robust Nonlinear Control Technology for High-Agility Missile Interceptors. *Optimal Synthesis Inc*. Report No. 005, Prepared Under NSWCDD Contract No.

Menon, P. K., & Iragavarapu, V. R. (1998). Adaptive Techniques for Multiple Actuator Blending. *AIAA Guidance, Navigation, and Control Conference*. Boston, MA.

Menon, P. K., Iragavarapu, V. R., & Ohlmeyer, E. J. (1999). Software Tools for Nonlinear Missile Autopilot Design. *AIAA Guidance, Navigation and Control Conference*. Portland, OR.

Menon, P. K., Cheng, V. H. L., Lam, T., Crawford, L. S., Iragavarapu, V. R. & Sweriduk, G. D. (2000a). Nonlinear synthesis tools for use with MATLAB®. Palo Alto, CA: Optimal Synthesis Inc.

Menon, P. K., Lam, T., Crawford, L. S., Cheng, V. H. L. (2000b). Real-Time, SDRE-Based Nonlinear Control Technology. *Optimal Synthesis Inc*. Final Prepared Under AFRL Contract No. F08630-99-C-0060, January.

Marino, R., & Tomei, P. (1995). *Nonlinear control design, geometric, adaptive & robust*. London: Prentice-Hall International.

Ohlmeyer, E. J. (1996). Root-mean-square miss distance of proportional navigation missile against sinusoidal target. *Journal of Guidance, Control, and Dynamics*, *19*(3), 563–568.

Siljak, D. D. (1991). *Decentralized control of complex systems*. New York, NY: Academic Press.

Wolovich, W. A. (1994). *Automatic control systems*. New York, NY: Harcourt-Brace.

Zarchan, P. (1995). Proportional navigation and weaving targets. *Journal of Guidance, Control and Dynamics*, *18*(5), 969–974.